An Activity-Based Infrared Glucuronide Trapping Probe for Imaging β-Glucuronidase Expression in Deep Tissues

Journal:	*Journal of the American Chemical Society*
Manuscript ID:	ja-2011-09335z
Manuscript Type:	Article
Date Submitted by the Author:	04-Oct-2011

Complete List of Authors:	Cheng, Ta-Chun; Kaohsiung Medical University, Graduate Institute of Medicine Roffler, Steve; Academia Sinica, Institute of Biomedical Sciences Tzou, Shey-Cherng; Kaohsiung Medical University, Department of Biomedical Science and Environmental Biology Chuang, Kuo-Hsiang; Kaohsiung Medical University, Department of Biomedical Science and Environmental Biology Su, Yu-Cheng; National Yang-Ming University, Graduate Institute of Microbiology and Immunology Chuang, Chih-Hung; National Cheng Kung University, Institutes of Basic Medical Sciences Kao, Chien-Han; Kaohsiung Medical University, Graduate Institute of Medicine Chen, Chien-Shu; China Medical University, School of Pharmacy Harn, I-Hong; Kaohsiung Medical University, Department of Biomedical Science and Environmental Biology Liu, Kuan-Yi; Chia Nan University of Pharmacy and Science, Department of Pharmacy Cheng, Tian-Lu; Kaohsiung Medical University, Department of Biomedical Science and Environmental Biology; Kaohsiung Medical University Hospital, Cancer Center Leu, Yu-Ling; Chia Nan University of Pharmacy and Science, Department of Pharmacy

An Activity-Based Infrared Glucuronide Trapping Probe for Imaging β-Glucuronidase Expression in Deep Tissues

Ta-Chun Cheng[1#], Steve R. Roffler[2#], Shey-Cherng Tzou[3], Kuo-Hsiang Chuang[3], Yu-Cheng Su[4], Chih-Hung Chuang[5], Chien-Han Kao[1], Chien-Shu Chen[6], I-Hong Harn[3], Kuan-Yi Liu[8], Tian-Lu Cheng[3,7*] and Yu-Ling Leu[8*]

[1]Graduate Institute of Medicine, Kaohsiung Medical University, Kaohsiung, Taiwan; [2]Institute of Biomedical Sciences, Academia Sinica, Taipei, Taiwan; [3]Department of Biomedical Science and Environmental Biology, Kaohsiung Medical University, Kaohsiung, Taiwan; [4]Graduate Institute of Microbiology and Immunology, National Yang-Ming University, Taipei, Taiwan; [5]Institutes of Basic Medical Sciences, National Cheng Kung University, Tainan, Taiwan; [6]School of Pharmacy, China Medical University, Taichung, Taiwan; [7]Cancer Center, Kaohsiung Medical University Hospital, Kaohsiung, Taiwan; [8]Department of Pharmacy, Chia Nan University of Pharmacy and Science, Tainan, Taiwan

[#]equal contribution

*Correspondance:

Dr. Tian-Lu Cheng, Department of Biomedical and Environmental Biology, Kaohsiung Medical University, No. 100, Shiquan 1st Road, Kaohsiung City 80708, Taiwan. Phone: 886-7-3121101-2360, Fax: 886-7-3227508, E-mail: tlcheng@kmu.edu.tw.

Dr. Yu-Ling Leu, Department of Pharmacy, Chia Nan University of Pharmacy and Science, No. 60, Section 1, Erh-Ren Road, Tainan City 71710, Taiwan. Phone: 886-6-2664911-2236, Fax: 886-6-2667318, E-mail: yulin@mail.chna.edu.tw

Abstract

Infrared (IR) glucuronide probes that can track β-glucuronidase (βG) activity in vivo would substantially aid preclinical development of βG-based imaging and therapies. However, IR glucuronide probes are not yet available. Here, we developed IR- and fluorescein (FITC-) difluoromethyphenol-glucuronide trapping (TrapG) probes. Upon βG-mediated hydrolysis of the glucuronly bond of TrapG, a highly reactive alkylating group attaches the fluorochrome to nucleophilic moieties nearby βG. FITC-TrapG was selectively trapped on purified E. Coli βG (eβG) or βG-expressing CT26 cells (CT26/mβG), but not on control bovine serum albumin (BSA) or CT26 cell in vitro. βG-activated FITC-TrapG did not interfere with βG activity and was found to label bystander proteins near βG. For in vivo imaging, both FITC-TrapG and IR-TrapG specifically targeted subcutaneous CT26/mβG tumors. However, only IR-TrapG could image CT26/mβG tumors transplanted deep in the liver. Thus IR-TrapG may provide a valuable tool for imaging βG activity to optimize βG-based imaging and therapies.

Introduction

β-glucuronidase (βG) has been widely used in prodrug-activating therapies[1-4] and as a reporter gene to track the location of gene delivery vectors in preclinical studies[5-8]. The ability to image βG activity *in vivo* will greatly aid in the optimization of βG-based imaging and therapies. However, most βG probes are suitable only for *in vitro* studies but not yet available for *in vivo* imaging of βG activity. For example, Naphthol AS-BI β-D-glucuronide[9,10], p-nitrophenyl-β-D-glucuronide (PNPG)[11] and 5-bromo-4-chloro-3-indolyl-β-D-glucuronic acid (X-GlcA, X-Gluc)[12,13] are commonly used to detect βG activity in cultured cells and in histological sections. However, these colorimetric substrates have poor sensitivities and relatively narrow dynamic ranges. A wide variety of fluorogenic substrates, such as fluorescein di-β-D-glucuronide (FDGlcU)[7] and 4-methylumbelliferyl β-D-glucuronide (MU-GlcA)[12] have been developed to increase detection sensitivity. Our pervious study demonstrated that fluorescein di-β-D-glucuronide (FDGlcU) can assess βG activity *in vitro* and *in vivo*.[7] The penetrability of the FDGlcU spectrum, however, is insufficient to monitor βG-expressing tumors in deep organs in a living animal. Moreover, the signal generated with the FDGlcU probe rapidly diffuses away from βG-expressing sites and thus only allows imaging of subcutaneous βG-expressing tumors over a relatively narrow time window.[7]

Development of infrared glucuronide probes (>800 nm) may facilitate imaging of deep tissues and improve imaging resolution for βG.

In this study, we developed an infrared (IR) fluorescent difluoromethyphenol-glucuronide (TrapG) probe. βG-mediated hydrolysis of the glucuronly bond generates a highly reactive quinine methide intermediate that can attach the fluorochrome to nucleophilic side chains near βG-expressing sites (**Figure 1**). The IR-TrapG probe is advantageous in that it provides a specific and direct "activity-based" enzyme profile for βG. In addition, the high penetrability of IR signals could make this strategy useful for deep tissue imaging.[14-16] Here we report the design and synthesis of two fluorescent probes for βG: IR-TrapG and fluorescein FITC-TrapG. We first examined the specificity of these trapping probes by incubating FITC-TrapG with recombinant *E. coli* βG (eβG) or βG-expressing mouse colon cancer cells (CT26/mβG) *in vitro*. We investigated whether alkylation by activated FITC-TrapG affects βG activity and whether FITC-TrapG could label bystander proteins in the vicinity of βG activity. Finally, we examined whether IR-TrapG or FITC-TrapG could specifically image the location of βG-expressing CT26 tumors transplanted under the skin or deep in the livers of mice. IR-TrapG displays high tissue penetrability and may be a useful tool for tracking βG activity *in vivo* and for optimizing preclinical βG-based therapies and imaging

systems.

Results

Development of glucuronide trapping probes

To develop novel glucuronide trapping probes, FITC and IR were linked to a glucuronide group via a difluoromethylphenol trapping moiety, to from FITC-TrapG and IR-TrapG. The glucuronide group acts as a hydrophilic and cell impermeable βG substrate. βG-mediated hydrolysis of the glucuronly bond in the probe exposes the quinine methide group which can crosslink FITC or IR to nearby nucleophiles (Figure 1). The design and synthesis of FITC-TrapG and IR-TrapG are shown in **Schemes 1-5.** Details of synthesis are described in the experimental section and supporting information.

Characterization of glucuronide trapping probes *in vitro*

To examine if βG can specifically activate FITC-TrapG and expose the reactive alkylating group *in vitro*, graded amounts of FITC-TrapG were incubated with either purified E. coli βG (eβG) or bovine serum albumin (BSA) absorbed in microtiter plates. FITC that became attached to proteins in the wells was then detected using an anti-FITC antibody. Figure 2A shows that absorbance at 405 nm increased with the concentration of the probe added to eβG. Conversely, incubation of FITC-TrapG with BSA did not result in accumulation of FITC in the wells. Similarly, mouse βG (mβG) tethered on the surface

of CT26 cells also activated FITC-TrapG and retained FITC (Figure 2B). No color development was noted after addition of FITC-TrapG to parental CT26 cells. These results indicate that the glucuronide trapping probes were specifically activated by βG and stably retained. Furthermore, activated FITC-TrapG did not hamper βG activity since 100% enzymatic activity was maintained even at the highest concentration (40 μg/mL) of FITC-TrapG (Figure 2C and 2D). We conclude that activated FITC-TrapG can be retained at sites of βG activity without affecting its enzymatic activity.

Conceptually, activated FITC-trapG probe can alkylate any nucleophile in close proximity to βG. To test whether the activated probes could label bystander nucleophiles, we added FITC-TrapG to a mixture of eβG and BSA in solution. Addition of FITC-TrapG resulted in labeling of FITC groups on both eβG (74 kDa) and BSA (66 kDa) (Figure 3). In the absence of βG-mediated activation, FITC-TrapG did not label the control protein BSA. We conclude that activated FITC-TrapG can label bystander nucleophiles in the vicinity of βG enzyme activity.

Imaging of βG activity in subcutaneous tumors

To examine whether the glucuronide trapping probes can specifically detect βG activity *in vivo*, we intravenously injected FITC-TrapG to BALB/c nude mice bearing

subcutaneous CT26 or CT26/mβG tumors. Fluorescent signals were measured in live mice with a noninvasive optical imaging system. Figure 4A shows that the fluorescent intensity (defined as photons/sec/cm^2/sr) in the CT26/mβG tumors were greater than in the control CT26 tumors at 24, 48 and 72 hours, respectively. In line with the imaging results, FITC-derived fluorescence was retained in CT26/mβG tumors but not control CT26 tumors, which was consistent with X-GlcA staining for βG activity (Figure 4B). Similarly, IR-TrapG could specifically label βG-expressing cells *in vitro* (Figure 5A) and subcutaneous βG-expressing tumors *in vivo*. Cell-associated IR intensity was 2.4, 2.6, and 2.8-fold greater in CT26/mβG cells than in control CT26 cells (Figure 5A). IR signals also increased over time in subcutaneous CT26/mβG tumors as compared to the control CT26 tumors at 24, 48, and 72 hours (Figure 5B). We conclude that the glucuronide trapping probes can image βG activity in live animals.

Imaging of βG activity in tumors transplanted in livers

Deep tissues present a major technical challenge to optical imaging. To test whether IR-TrapG can be used for deep tissue imaging, we injected IR-TrapG to BALB/c nude mice that had CT26 or CT26/mβG tumors transplanted under their liver capsule. FITC-TrapG was also injected in separate mice with liver tumors. Figure 6A shows that

IR signals were detected in live mice bearing CT26/mβG tumors in their liver. Consistent with the noninvasive imaging results, significantly stronger IR signals were recorded in livers isolated from mice bearing CT26/mβG tumor transplants than in mice bearing control CT26 tumors. On the contrary, no FITC signal was detected in live mice; FITC signals were only detected when animals were killed and livers were placed directly under the detector (Figure 6B). Collectively, these results demonstrate that IR-TrapG can detect βG activity in deep tissues.

Discussion

We have developed an IR glucuronide trapping probe (IR-TrapG) for *in vivo* imaging of βG expression in deep tissues. βG-mediated hydrolysis of the glucuronyl bond of IR-TrapG led to crosslinking of the probe onto nearby nucleophiles at βG-expressing sites. The *in vitro* analyses demonstrated that this novel glucuronide trapping probe did not affect βG activity and the activated probe could label bystander proteins. The high penetrability of IR signals through tissues renders this probe especially useful for noninvasive optical imaging of βG expression in deep tissues.

IR fluorescent dyes are useful for biomedical studies. IR fluorochromes (700 nm~900 nm) have high signal/background ratios and penetrate tissues better than those with shorter wavelengths.[17-19] A β-galatosidase (LacZ) activated far red probe (DDOAG, 659nm) was reported to allow non-invasive monitoring of the expression and activity of LacZ *in vivo*.[20] Moreover, a PEGylated near-IR probe (PEG-NIR797, 797nm) could detect lung metastasis *in vivo*.[21] Adams and colleagues also reported that an IR Dye (800nm) conjugated epidermal growth factor produced better imaging of EGF receptor positive tumors than Cy5.5 (710nm).[22] In this report, we demonstrate that IR-TrapG (820nm), but not FITC-TrapG, can be used to visualize βG-expressing tumors in deep tissues (liver).

Activity-based probes have gained marked success for *in vivo* profiling of enzymatic activities including proteases[19,23], thymidine kinase[24,25], and galatosidase[20,26]. This concept depends heavily on the specific binding of the probe to the active site of the target enzyme. In most cases, activity-based probes irreversibly inactivate the target enzyme. By contrast, enzymatic activation of noninhibitory probes leads to signal amplification and thus improves detection. In addition, noninhibitory imaging probes do not interfere with therapeutic efficiency of enzyme-based prodrug therapies. Difluoromethylphenol has been demonstrated to display trapping activity after enzymatic activation,[27] but does not irreversibly inactivate enzymes.[28] Our glucuronide trapping probe does not appear to inhibit βG activity, which should enhance imaging by continuous activation. As many glucuronide antitumor prodrugs have been developed, such as 9-aminocamptothecin glucuronide (9ACG)[29] and p-hydroxyaniline mustard glucuronide (BHAMG)[30], to selectively kill βG over-expressing cancers[29,31], the glucuronide trapping probes may be useful for (1) screening βG over-expressing tumors and, (2) monitoring anti-cancer efficacy by glucuronide prodrugs in personalized therapy.

The trapping moiety (difluoromethylphenol) may be a versatile linker for multiple imaging systems because difluoromethylphenol could be, at least conceptually, coupled

to other imaging probes to detect βG activity. In this report, we have demonstrated that difluoromethylphenol could be conjugated to two fluorescent probes (FITC and IR-820) for optical imaging. Following derivative chemical principles, difluoromethyphenol is expected to be able to link a glucuronide group to different imaging agents, such as 1,4,7-tricarboxymethylene-1,4,7,10-tetraazacyclododecane (DO3A)[32] and 1,4,7,10-tetraazacyclododecane-*N*,*N*',*N*'',*N*'''-tetraacetic acid (DOTA)[25] for magnetic resonance imaging, or radioiodinated tyramine[4] and fluoroethylamine[33] for nuclear imaging (PET and SPECT). Development of βG-specific probes along these lines may further broaden selection of tools to monitor βG expression *in vivo*. Furthermore, the trapping strategy may hold great potential for developing a variety of novel imaging probes to detect other enzymes relevant to human diseases.

Conclusions:

The IR glucuronide trapping probe possesses several attractive attributes. The probe has high penetrability for noninvasive imaging of βG activity in deep tissues. The trapping moiety (difluoromethylphenol) does not inhibit βG activity, allowing enhancement of image intensity. The trapping strategy may be extended to other imaging systems or other enzymes. Based on these advantages, we believe that the glucuronide trapping probe may provide a valuable tool for imaging βG activity in preclinical studies.

Figures:

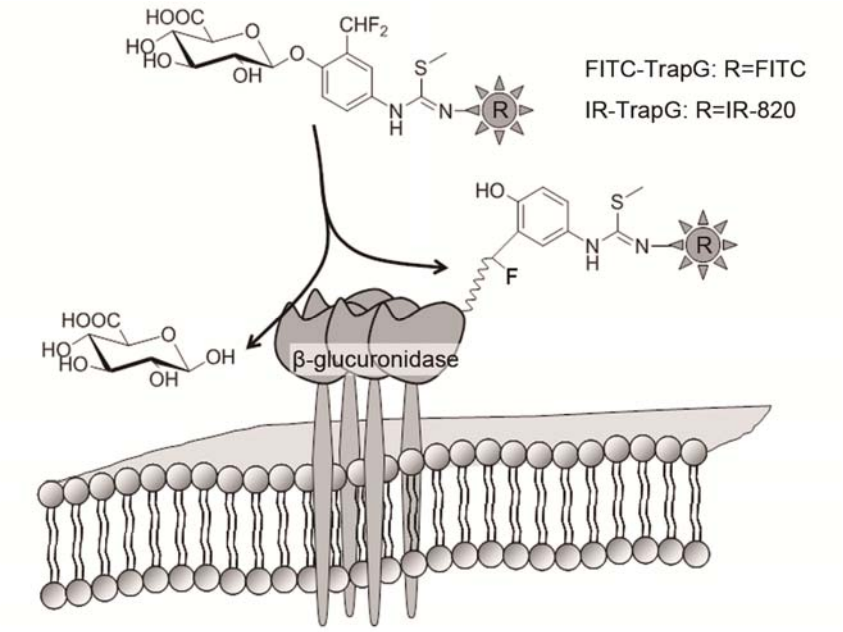

Figure 1. **Mechanism of the βG activity-based trapping probe.** Upon βG-mediated hydrolysis of the glucuronly bond, a highly reactive quinine methide intermediate is generated that leads to crosslinking of the probe to nearby nucleophiles.

Scheme 1. Chemical structure and synthesis of *methyl 1-O-(2-difloromethyl-4-amino)-β-D-glucopyranuronate*

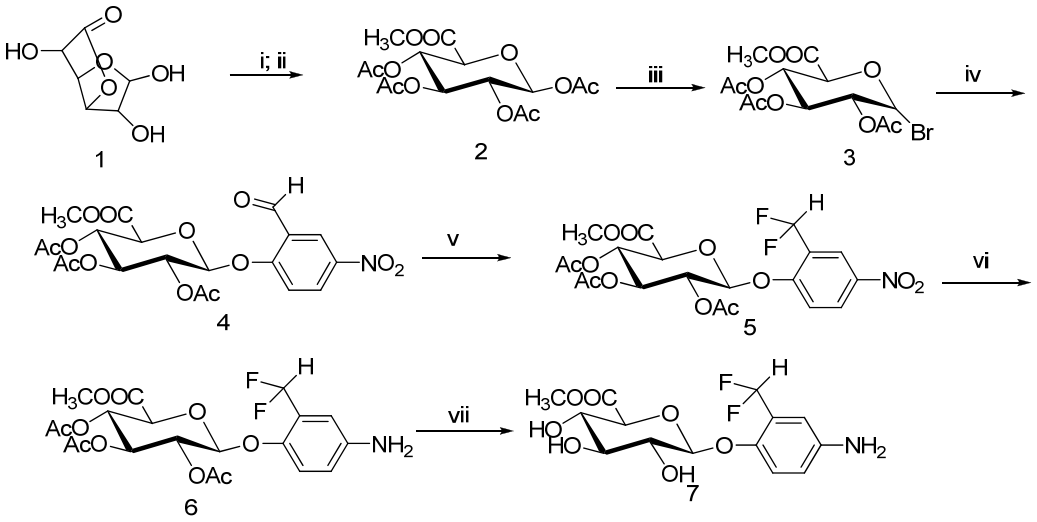

Scheme 2. Autodegradation of *N'-fluorescein–N"-[4-O-(methyl-2,3,4-tri-O-acetyl-β-D-glucopyranuronate)-3-difloromethylphenylthiourea*

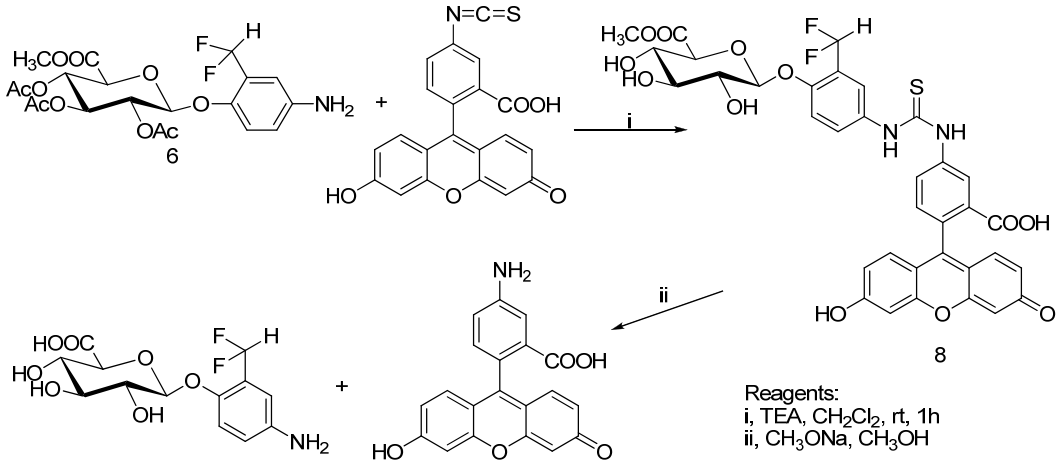

Scheme 3. Chemical structure and synthesis of *N'-fluorescene-N"-[4-O-(β-D-glucopyranuronate)-3-difloromethylphenyl-S-methyllthiourea* (FITC-TrapG)

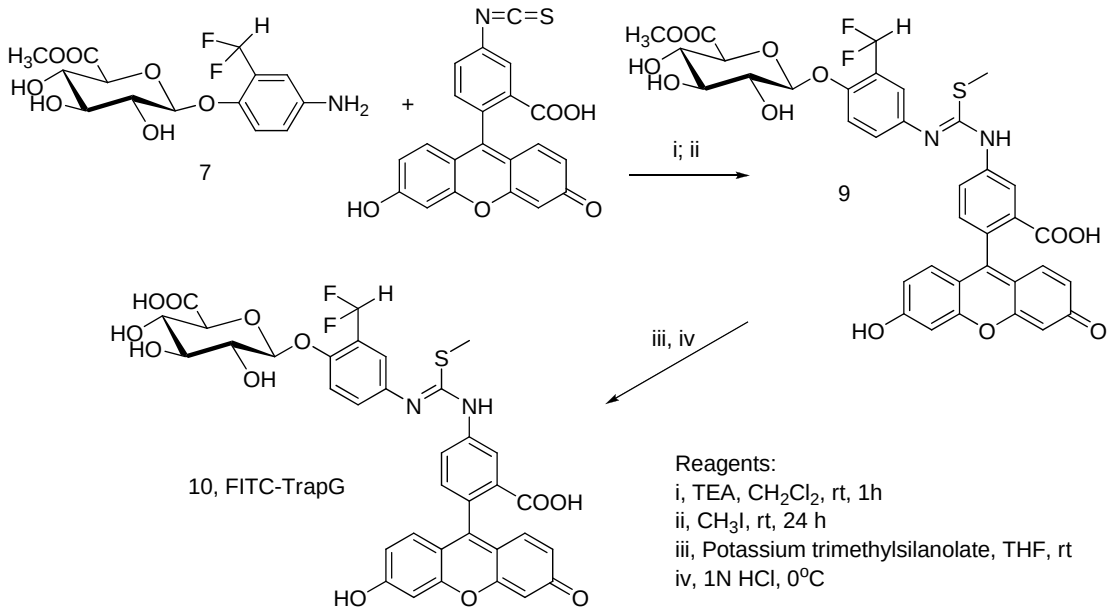

Scheme 4. Chemical structure and synthesis of IR-820.SPh.NCS

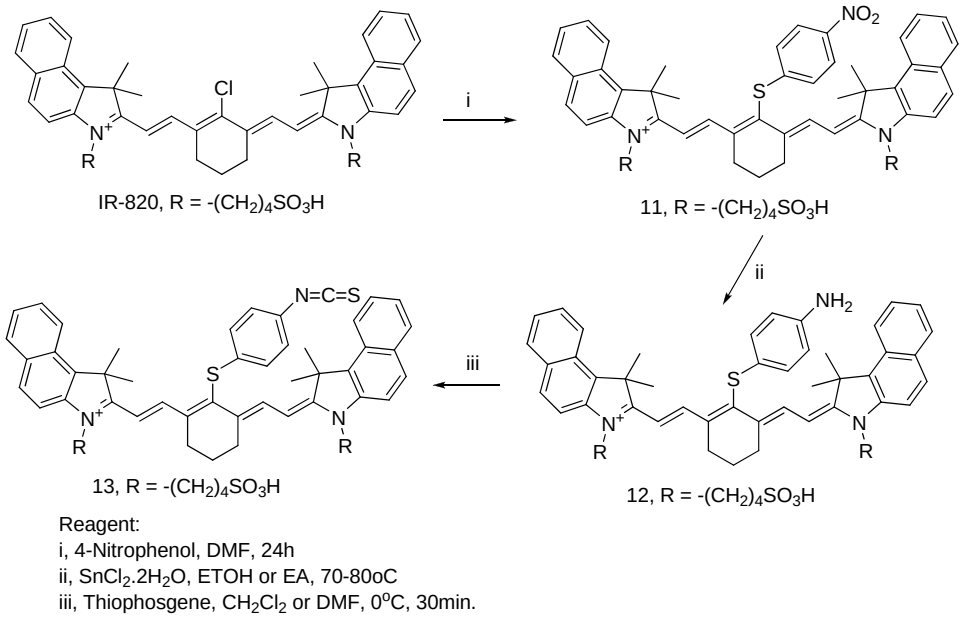

Scheme 5. Chemical structure and synthesis of *N'-(p-aminophenylthioether* of IR-820-*N"-[4-O-(β-D-glucopyranuronate)-3-difloromethylphenyl-S-methyllthiourea* (IR-TrapG)

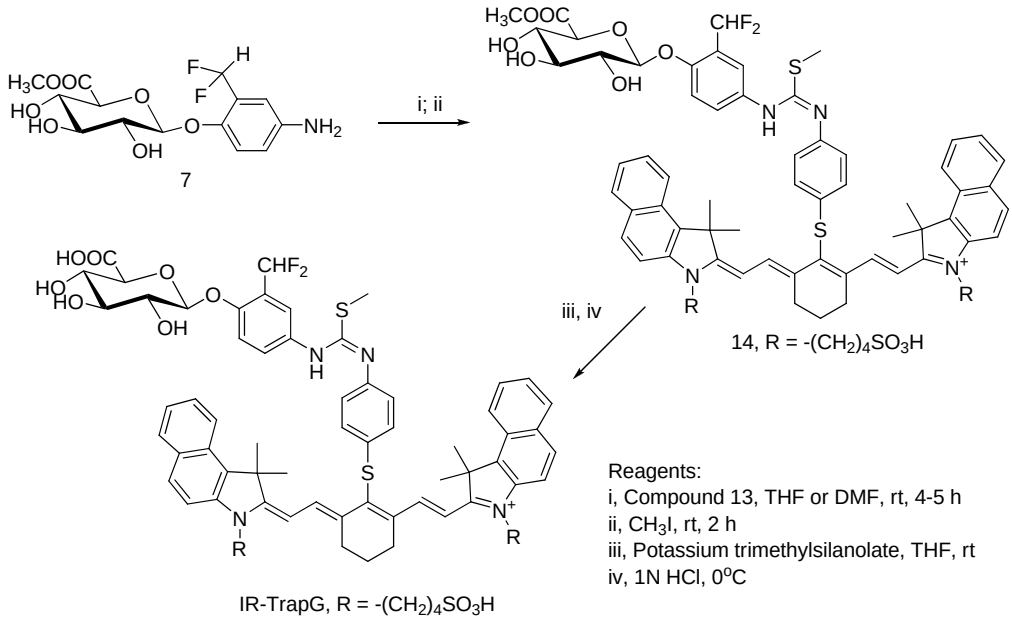

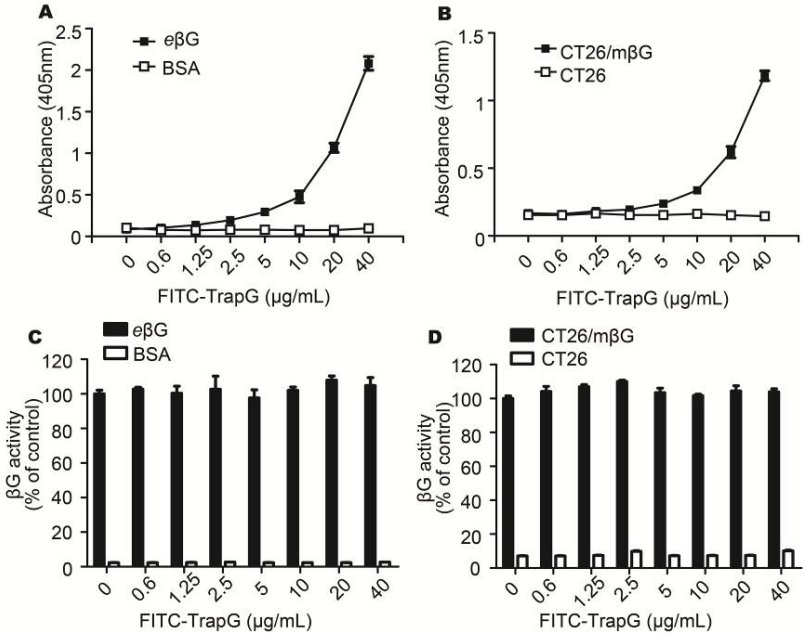

Figure 2. **βG-specific activation of FITC-TrapG *in vitro*.** Graded amounts of FITC-TrapG were incubated with (A) βG (filled squares) or BSA (open squares) or (B) CT26/mβG (filled squares) or CT26 (open squares) precoated in the wells of a microtiter plate. Activation and trapping of FITC-TrapG was determined by ELISA using an anti-FITC antibody. After FITC-TrapG treatment, βG activity was determined by hydrolysis of p-NPG substrate in (C) purified proteins (eβG, BSA) or (D) cells (CT26/mβG, CT26).

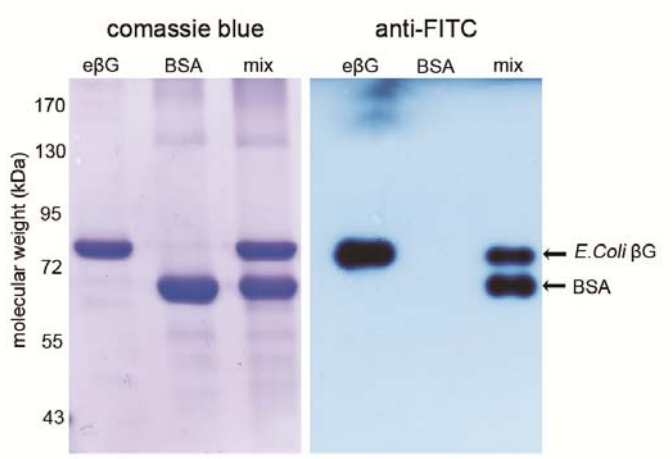

Figure 3. **Bystander trapping by FITC-TrapG.** FITC-TrapG was incubated with eβG, BSA or a mixture of eβG and BSA. Activation and trapping of FITC-TrapG to proteins was detected by Western blotting using an anti-FITC antibody (right panel). Protein loading was visualized by Coomassie blue staining (left panel)**.**

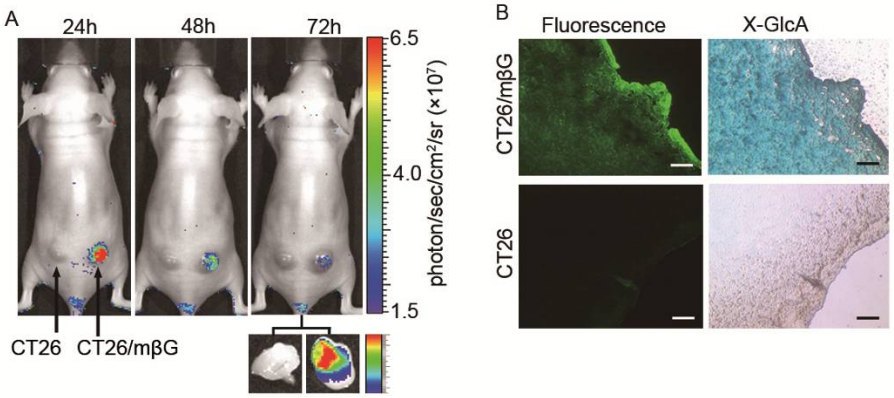

Figure 4. Specific activation of FITC-TrapG *in vivo*. FITC-TrapG was intravenously injected to BALB/c nude mice bearing CT26/mβG (right flank) and CT26 (left flank) tumors. (A) *In vivo* optical imaging of FITC-TrapG at 24, 28, 72 hours after probe injection. Tumor tissue was also harvested to confirm specific fluorescent signals. (B) CT26/mβG and CT26 tumors were resected at 24 hours after FITC-TrapG injection, stained with X-GlcA and examined under bright field and fluorescent field illumination. Scale bar: 100 μm.

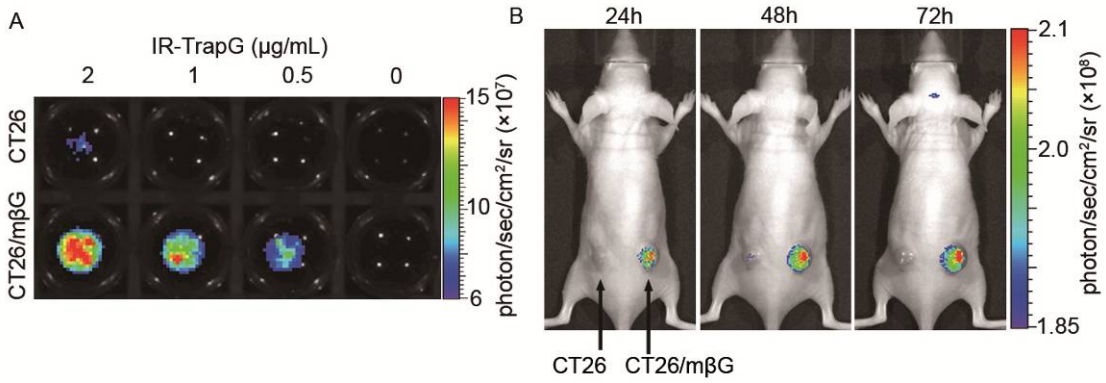

Figure 5. **Optical imaging using IR-TrapG.** (A) Optical imaging of CT26/mβG or CT26 cells (3×10^6/well) pretreated with 2, 1, 0.5, and 0 μg/ml of IR-TrapG. (B) Optical imaging of subcutaneous CT26/mβG and CT26 tumors in mice at 24, 28, 72 hours after probe injection.

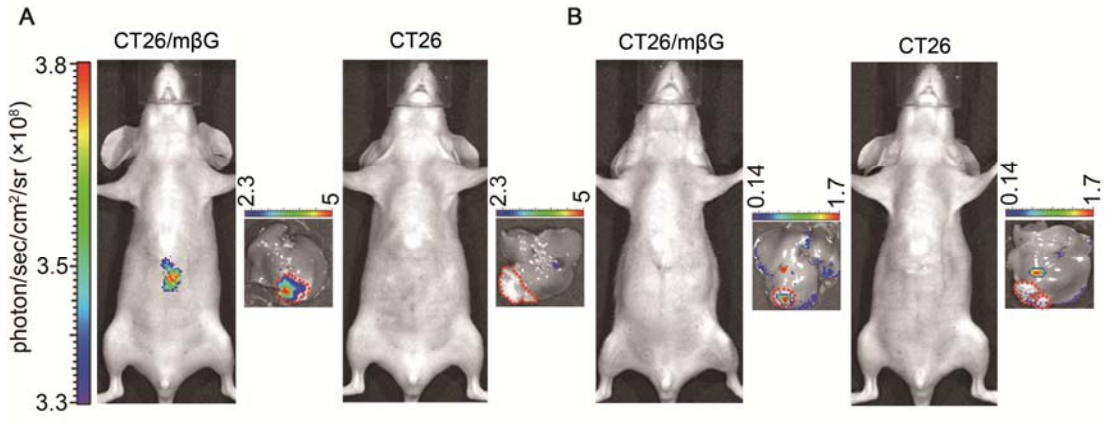

Figure 6. **Deep tissue imaging of βG-expressing tumors using IR-TrapG.** IR-TrapG or FITC-TrapG was injected into BALB/c mice bearing CT26 or CT26/mβG tumor transplants in livers. Noninvasive optical imaging of (A) IR-TrapG or (B) FITC-TrapG was performed at 24 hours after probe injection. Livers were harvested to confirm location of tumors and specificity of the fluorescent signal. Red dotted lines indicate tumor locations in the liver.

Experimental Section

Design and synthesis of FITC-TrapG and IR-TrapG

The detailed chemistry procedures are described in supporting information. To develop novel glucuronide trapping probes, FITC or IR was linked to a glucuronide group by a trapping moiety, difluoromethylphenol, to from FITC-TrapG or IR-TrapG as activity-based probes. FITC-TrapG and IR-TrapG were prepared from methyl 1-α-bromo-1-deoxy-2,3,4-tri-*O*-acetyl-β-D-glucopyranuronate (**3**) and 2-hydroxy-5-nitrobenzaldehyde using a previously published method for the synthesis of glucuronide derivates,[34] with minor modifications. The aldehyde group in **4** was fluorinated to a difluoromethyl group with diethylaminosulfur triflouride (DAST). The nitro group in **5** was reduced in a palladium-catalyzed reaction to obtain **6** (Scheme 1). For synthesis of FITC-TrapG, the aniline in **6** was reacted with fluorescein isothiocyanate (FITC) to obtain a methyl *O*-acetyl protected FITC-TrapG (**8**). However, when compound **8** was deprotected with sodium methoxide, the thiourea linkage was hydrolyzed (Scheme 2), indicating that the thiourea linkage is susceptible to hydrolysis at basic or physiological pH. We modified the synthesis pathway to enhance stability. The acetyl group in compound **6** was deprotected by sodium methoxide to give **7** (Scheme 1). The aniline in **7** was condensed with FITC, following by addition of methyl iodide (CH_3I)

to create a *S*-methyl pseudothiourea linkage[35] in FITC-TrapG (**9**). Next, **9** was deprotected with potassium trimethylsilanolate, followed by acidification with 1N HCl to obtain FITC-TrapG (**10**) (Scheme 3).

For synthesis of IR-TrapG, the fluorescein group in FITC-TrapG was replaced by an IR dye (IR-820). The commercial IR-820 chlorocyanine dye was condensed with p-nitrothiophenol by nucleophilic substitution to obtain compound **11**. The nitro group in **11** was reduced by $SnCl_2.2H_2O$ to generate an aminothioether dye, compound **12**. The amino group in **12** was reacted with thiophosgene to generate the isothiocyanate, compound **13** (Scheme 4). IR-TrapG was prepared from compound **7** which was reacted with isothiocyanate **13**, followed by addition of CH_3I to create the *S*-methyl pseudothiourea linkage of IR-TrapG (**14**). Next, compound **14** was deprotected with potassium trimethylsilanolate, followed by acidification by 1N HCl to obtain IR-TrapG (**15**) (Scheme 5).

Cells and mice

CT26 and CT26/mβG cells[7] were maintained in Dulbecco's minimal essential medium (DMEM) (Sigma-Aldrich, St Louis, MO, USA) supplemented with 10% bovine calf serum, 100 μg/ml penicillin and 100 μg/ml streptomycin at 37℃ in an atmosphere of 5%

CO_2. Female BALB/c nude (BALB/cAnN.Cg-Foxn1nu/CrlNarl) mice, 5~6 weeks old, were purchased from the National Laboratory Animal Center, Taiwan. The animal experiments were conducted in accordance with the standards set forth by the Kaohsiung Medical University Institutional Animal Care and Use Committee.

Specific activation of FITC-TrapG *in vitro*

Purified eβG (5 μg/well) and bovine serum albumin (5 μg/well) (Sigma-Aldrich) were coated overnight in 96 well microtiter plates in phosphate-buffered saline (PBS) (pH 8.0) and then blocked with 5% skin milk at room temperature for 2 hours. CT26/mβG and control CT26 cells were seeded at 1.5×10^5 cells/well in 96 well microtiter plates in culture medium overnight. FITC-TrapG was 2-fold serially diluted (starting from 40 μg/mL) in PBS, and then added to the proteins or cells at 37℃ for 1 hour. The plates were washed with PBS and then stained with a mouse anti-FITC antibody (Sigma-Aldrich), followed by a horseradish peroxidase-conjugated goat anti-mouse IgG antibody (Jackson ImmunoResearch Laboratories, West Grove, PA, USA). Following three washes with PBS, 2,2'-azino-bis(3-ethylbenzothiazoline-6-sulfonic acid) (ABTS) (Sigma-Aldrich) with 0.03% hydrogen peroxide (H_2O_2) (Sigma-Aldrich) was added to the wells, and color development was measured on a microplate reader (Molecular

Device, Menlo Park, CA) at OD 405 nm.

βG enzymatic activity after FITC-TrapG treatment

To test whether activated FITC-TrapG inactivates βG enzyme activity, plate-bound eβG or CT26/mβG cells were incubated with FITC-TrapG as described above. Following proper washing in PBS, p-nitrophenyl β-D-glucuronide (PNPG) (Sigma-Aldrich) was added to the plates. Color development was measured on a microplate reader at OD 405 nm.

Bystander trapping of FITC-TrapG

Purified eβG, BSA, or a mixture of eβG/BSA (50 μg/each in PBS) were incubated with FITC-TrapG (40 μg/ml) at 37℃ for 1 h. Proteins were precipitated by cold acetone and centrifuged at 12,000xg for 15 min, then electrophoresed on a 10% reducing SDS-PAGE (0.5 μg/lane) and transferred to a NC membrane (Pall, Port Washington, NY, USA). Membranes were blocked with 5% skim milk in PBS. FITC attached on proteins was detected by immunoblotting using a mouse anti-FITC antibody (Sigma-Aldrich), a horseradish peroxidase-conjugated goat anti-mouse IgG antibody (Jackson ImmunoResearch Laboratories) and an enhanced chemiluminescence kit (Millipore,

Billerica, MA, USA).

***In vitro* imaging of IR-TrapG**

CT26 and CT26/mβG cells (3×10^6) were stained with 2, 1, 0.5 or 0 μg/ml IR-TrapG in PBS containing 0.05% BSA at 37℃ for 2 h. The cells were washed with PBS 3 times, and the fluorescence was detected on an IVIS50 optical imaging system (excitation: 760nm, emission: 835 nm, Caliper Life Sciences, MA, USA).

***In vivo* imaging of FITC-TrapG and IR-TrapG**

BALB/c nude mice (n=3) bearing CT26 (in left flanks) and CT26/mβG (in right flanks) tumors (50-100 mm^3) were intravenously injected with 500 μg/mouse of FITC-TrapG or 100 μg/mouse of IR-TrapG in 100 μL PBS. Tumor-associated fluorescence was recorded on an IVIS50 at 24, 48 and 72 hours after probe injection. We also tested 100 μg/mouse of FITC-TrapG, but there was no significant difference (data not shown).

Histological analysis

Tumors were excised at 24 hours after FITC-TrapG injection, embedded in OCT compound (Tissue-Tek, CA, USA) at −80℃, and sectioned into 10 μm slices. Adjacent

tumor sections were stained for βG activity with the β-glucuronidase Reporter Gene Staining Kit (Sigma-Aldrich). The sections were viewed in bright field and fluorescence modes on an Eclipse TE2000-U Inverted Microscope (Nikon, Tokyo, Japan).

Tumor transplantation into liver and tumoral imaging using FITC-TrapG or IR-TrapG

BALB/c nude mice were anesthetized with ketamine/xylazine (135 mg/kg; 15 mg/kg) and abdomen cavities were surgically opened. 0.1 × 0.2 cm pieces of CT26/βG or CT26 tumors were transplanted under the capsule of the livers (n=3 for each group). One week after the transplantation, mice were intravenously injected with 500 μg/mouse of FITC-TrapG or 100 μg/mice of IR-TrapG in 100 μL PBS. Whole body fluorescent signals were recorded on an IVIS50 optical imaging system at 24 hours after probe injection. After noninvasive imaging, livers were harvested and placed directly under the detector of an IVIS50 system to reaffirm the location of tumors.

Supporting information

The detailed chemistry procedures and nuclear magnetic resonance (NMR) data of FITC- and IR- TrapG are described in supporting information. This material is available free of

charge via the Internet at http://pubs.acs.org.

Acknowledgements

This work was supported by grants from the National Research Program for Biopharmaceuticals, National Science Council, Taipei, Taiwan (NSC 100-2325-B-037-001-), Academia Sinica (AS-98-TP-B09) and the Department of Health, Executive Yuan, Taiwan (DOH100-TD-N-111-010 , DOH100-TD-C-111-002).

References:

(1) Sperker, B.; Werner, U.; Murdter, T. E.; Tekkaya, C.; Fritz, P.; Wacke, R.; Adam, U.; Gerken, M.; Drewelow, B.; Kroemer, H. K. *Naunyn Schmiedebergs Arch Pharmacol* **2000**, *362*, 110.

(2) de Graaf, M.; Boven, E.; Scheeren, H. W.; Haisma, H. J.; Pinedo, H. M. *Curr Pharm Des* **2002**, *8*, 1391.

(3) Chen, X.; Wu, B.; Wang, P. G. *Curr Med Chem Anticancer Agents* **2003**, *3*, 139.

(4) Juan, T. Y.; Roffler, S. R.; Hou, H. S.; Huang, S. M.; Chen, K. C.; Leu, Y. L.; Prijovich, Z. M.; Yu, C. P.; Wu, C. C.; Sun, G. H.; Cha, T. L. *Clin Cancer Res* **2009**, *15*, 4600.

(5) Jefferson, R. A.; Burgess, S. M.; Hirsh, D. *Proc Natl Acad Sci U S A* **1986**, *83*, 8447.

(6) Platteeuw, C.; Simons, G.; de Vos, W. M. *Appl Environ Microbiol* **1994**, *60*, 587.

(7) Su, Y. C.; Chuang, K. H.; Wang, Y. M.; Cheng, C. M.; Lin, S. R.; Wang, J. Y.; Hwang, J. J.; Chen, B. M.; Chen, K. C.; Roffler, S.; Cheng, T. L. *Gene Ther* **2007**, *14*, 565.

(8) Tzou, S. C.; Roffler, S.; Chuang, K. H.; Yeh, H. P.; Kao, C. H.; Su, Y. C.; Cheng, C. M.; Tseng, W. L.; Shiea, J.; Harm, I. H.; Cheng, K. W.; Chen, B. M.; Hwang, J. J.; Cheng, T. L.; Wang, H. E. *Radiology* **2009**, *252*, 754.

(9) Dolbeare, F. A.; Phares, W. *J Histochem Cytochem* **1979**, *27*, 120.

(10) Prosperi, E.; Raap, A. K. *Histochem J* **1982**, *14*, 689.

(11) Brot, F. E.; Bell, C. E., Jr.; Sly, W. S. *Biochemistry* **1978**, *17*, 385.

(12) Gallagher, S. R. *GUS protocols : using the GUS gene as a reporter of gene expression*; Academic Press: San Diego, 1992.

(13) Jefferson, R. A. *Nature* **1989**, *342*, 837.

(14) Weissleder, R. *Nat Biotechnol* **2001**, *19*, 316.

(15) Ye, Y.; Li, W. P.; Anderson, C. J.; Kao, J.; Nikiforovich, G. V.; Achilefu, S. *J Am Chem Soc* **2003**, *125*, 7766.

(16) Xing, B.; Khanamiryan, A.; Rao, J. *J Am Chem Soc* **2005**, *127*, 4158.

(17) Kovar, J. L.; Simpson, M. A.; Schutz-Geschwender, A.; Olive, D. M. *Anal Biochem* **2007**, *367*, 1.

(18) Ntziachristos, V.; Bremer, C.; Weissleder, R. *Eur Radiol* **2003**, *13*, 195.

(19) Mahmood, U.; Weissleder, R. *Mol Cancer Ther* **2003**, *2*, 489.

(20) Tung, C. H.; Zeng, Q.; Shah, K.; Kim, D. E.; Schellingerhout, D.; Weissleder, R. *Cancer Res* **2004**, *64*, 1579.

(21) Chuang, K. H.; Wang, H. E.; Cheng, T. C.; Tzou, S. C.; Tseng, W. L.; Hung, W. C.; Tai, M. H.; Chang, T. K.; Roffler, S. R.; Cheng, T. L. *J Nucl Med* **2010**, *51*, 933.

(22) Adams, K. E.; Ke, S.; Kwon, S.; Liang, F.; Fan, Z.; Lu, Y.; Hirschi, K.; Mawad, M. E.; Barry, M. A.; Sevick-Muraca, E. M. *J Biomed Opt* **2007**, *12*, 024017.

(23) Zhu, L.; Xie, J.; Swierczewska, M.; Zhang, F.; Quan, Q.; Ma, Y.; Fang, X.; Kim, K.; Lee, S.; Chen, X. *Theranostics* **2011**, *1*, 18.

(24) Bading, J. R.; Shields, A. F. *J Nucl Med* **2008**, *49 Suppl 2*, 64S.

(25) Gross, S.; Piwnica-Worms, D. *Cancer Cell* **2005**, *7*, 5.

(26) Kamiya, M.; Kobayashi, H.; Hama, Y.; Koyama, Y.; Bernardo, M.; Nagano, T.; Choyke, P. L.; Urano, Y. *J Am Chem Soc* **2007**, *129*, 3918.

(27) Janda, K. D.; Lo, L. C.; Lo, C. H.; Sim, M. M.; Wang, R.; Wong, C. H.; Lerner,

R. A. *Science* **1997**, *275*, 945.

(28) Hanson, S. R.; Whalen, L. J.; Wong, C. H. *Bioorg Med Chem* **2006**, *14*, 8386.

(29) Prijovich, Z. M.; Chen, B. M.; Leu, Y. L.; Chern, J. W.; Roffler, S. R. *Br J Cancer* **2002**, *86*, 1634.

(30) Wang, S. M.; Chern, J. W.; Yeh, M. Y.; Ng, J. C.; Tung, E.; Roffler, S. R. *Cancer Res* **1992**, *52*, 4484.

(31)Murdter, T. E.; Friedel, G.; Backman, J. T.; McClellan, M.; Schick, M.; Gerken, M.; Bosslet, K.; Fritz, P.; Toomes, H.; Kroemer, H. K.; Sperker, B. *J Pharmacol Exp Ther* **2002**, *301*, 223.

(32) Duimstra, J. A.; Femia, F. J.; Meade, T. J. *J Am Chem Soc* **2005**, *127*, 12847.

(33) Antunes, I. F.; Haisma, H. J.; Elsinga, P. H.; Dierckx, R. A.; de Vries, E. F. *Bioconjug Chem* **2010**, *21*, 911.

(34) Leu, Y. L.; Roffler, S. R.; Chern, J. W. *J Med Chem* **1999**, *42*, 3623.

(35) Zheng, W.; Papiernik, S. K.; Guo, M.; Yates, S. R. *Environ Sci Technol* **2004**, *38*, 1188.

Table of Contents Graphic

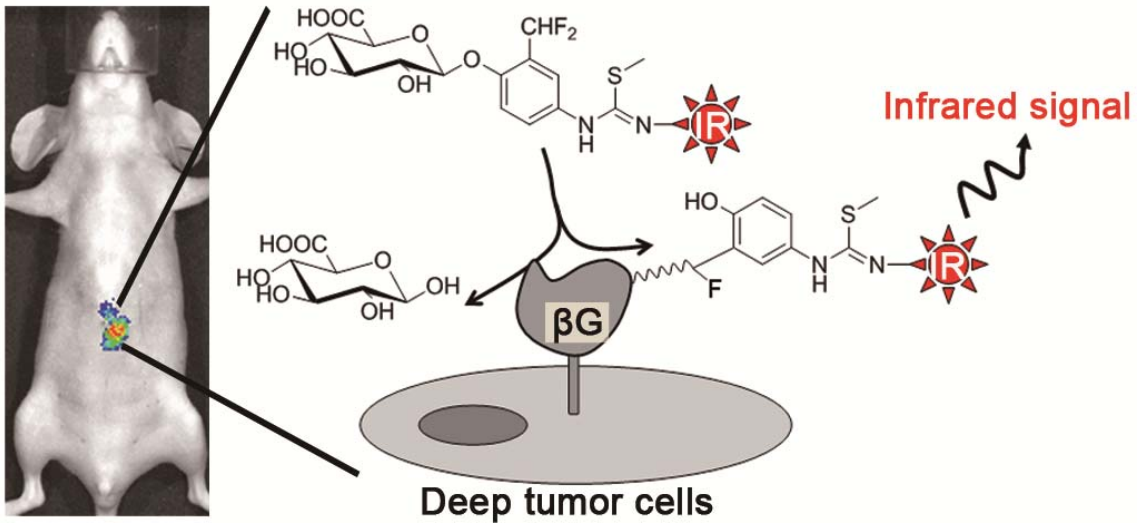

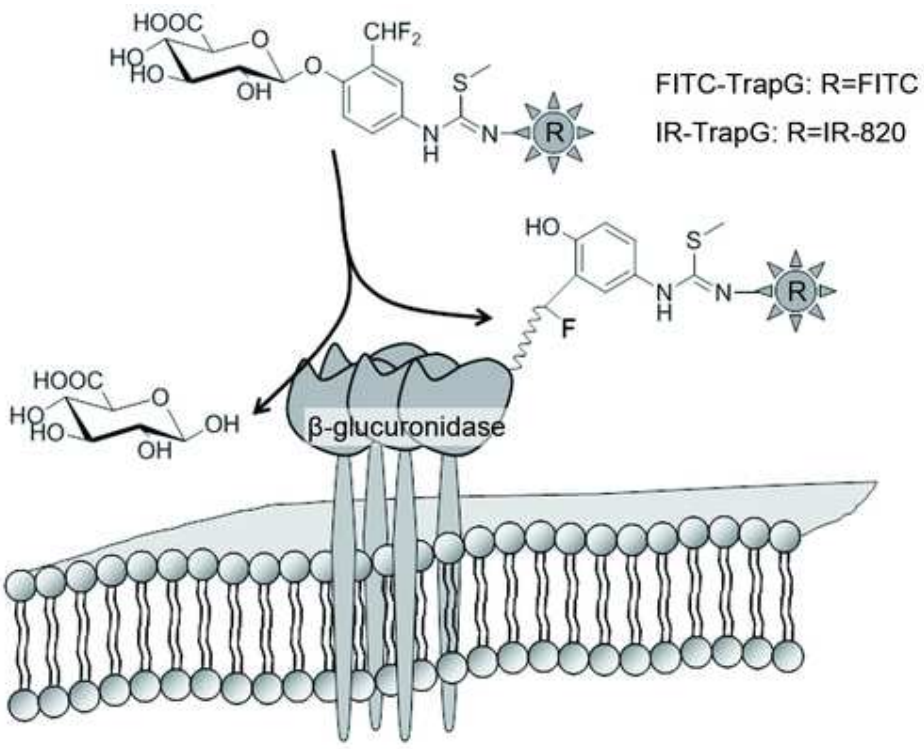

Figure 1. Mechanism of the βG activity-based trapping probe. Upon βG-mediated hydrolysis of the glucuronly bond, a highly reactive quinine methide intermediate is generated that leads to crosslinking of the probe to nearby nucleophiles.
44x33mm (300 x 300 DPI)

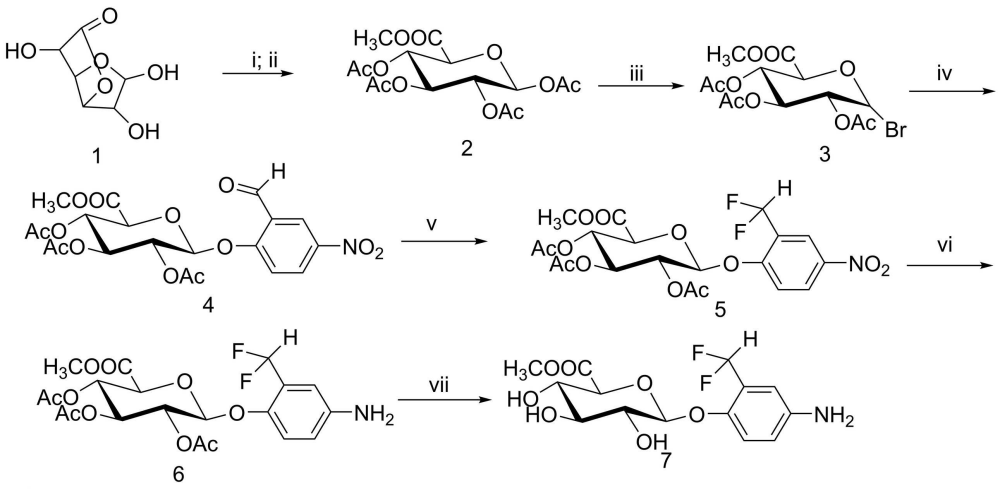

Reagents:
i, Sodium methoxide, MeOH, rt, 1 h.
ii, $HClO_4$, acetic anhydride, rt, 24 h.
iii, $TiBr_4$, CH_2Cl_2, rt, 24 h.
iv, 2-Hydroxy-5-nitrobenzaldehyde, Ag_2O, CH_3CN, rt, 24 h.
v, DAST, CH_2Cl_2
vi, 10% Pd/C, H_2, EA: MeOH(9:1)
vii, CH_3ONa, CH_3OH.

Scheme 1. Chemical structure and synthesis of methyl 1-O-(2-difloromethyl-4-amino)-β-D-glucopyranuronate
109x73mm (600 x 600 DPI)

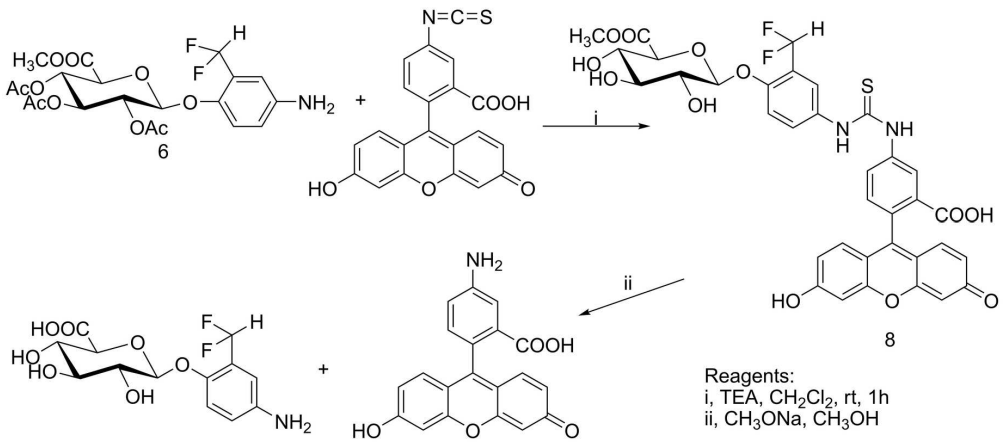

Scheme 2. Autodegradation of N'-fluorescein–N"-[4-O-(methyl-2,3,4-tri-O-acetyl-β-D-glucopyranuronate)-3-difloromethylphenylthiourea
77x34mm (600 x 600 DPI)

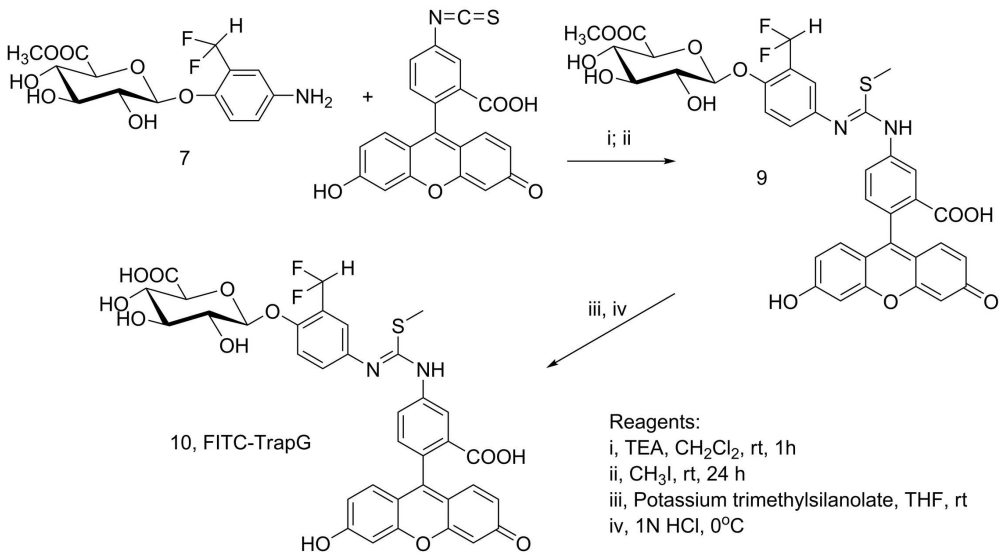

Scheme 3. Chemical structure and synthesis of N'-fluorescene-N"-[4-O-(β-D-glucopyranuronate)-3-difloromethylphenyl-S-methyllthiourea (FITC-TrapG)
96x53mm (600 x 600 DPI)

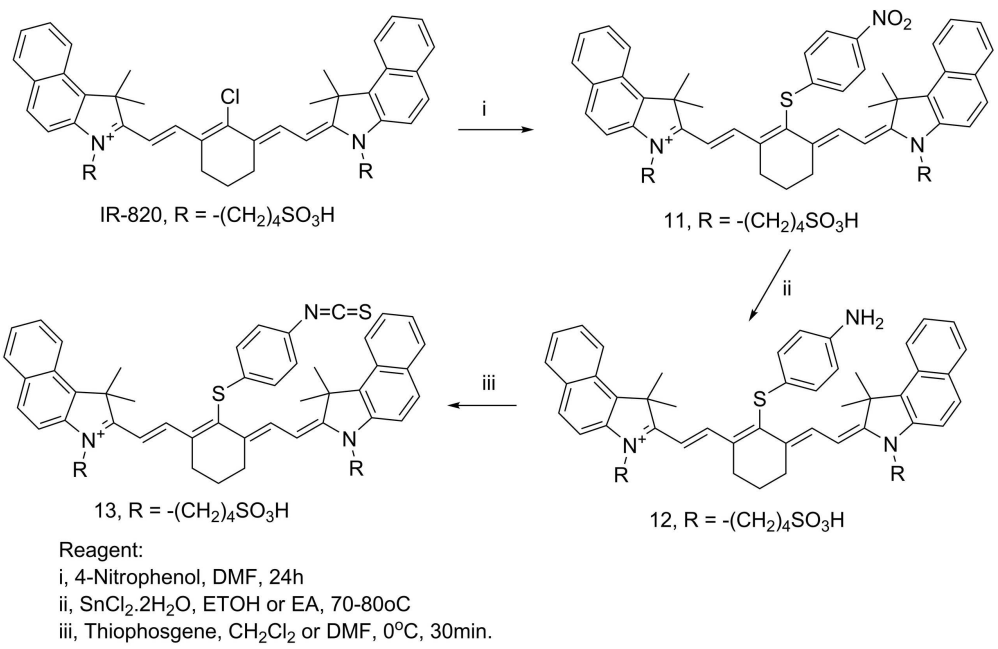

Scheme 4. Chemical structure and synthesis of IR-820.SPh.NCS
108x69mm (600 x 600 DPI)

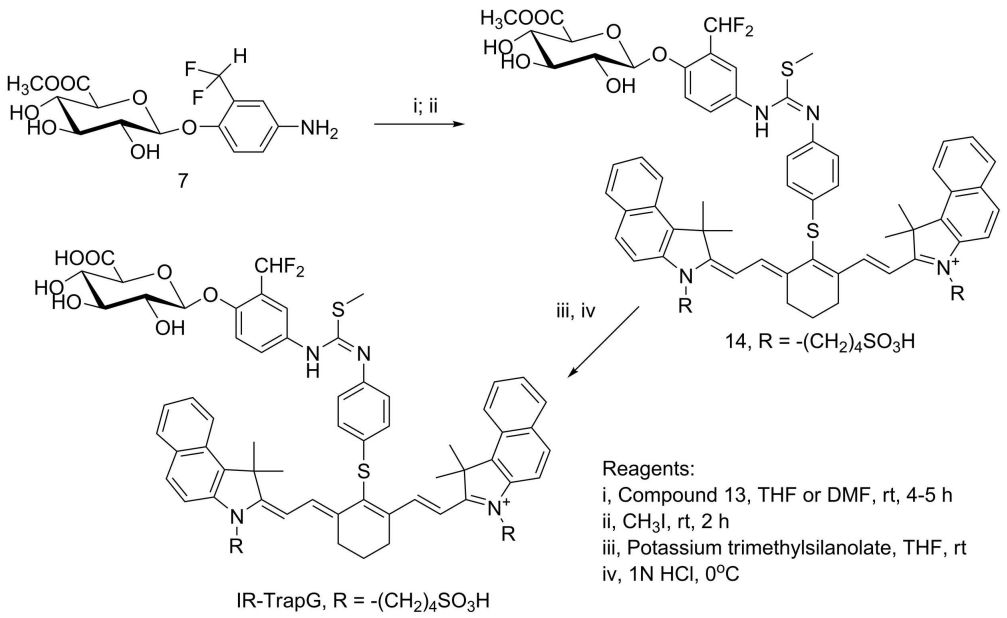

Scheme 5. Chemical structure and synthesis of N′-(p-aminophenylthioether of IR-820-N″-[4-O-(β-D-glucopyranuronate)-3-difloromethylphenyl-S-methyllthiourea (IR-TrapG)
105x64mm (600 x 600 DPI)

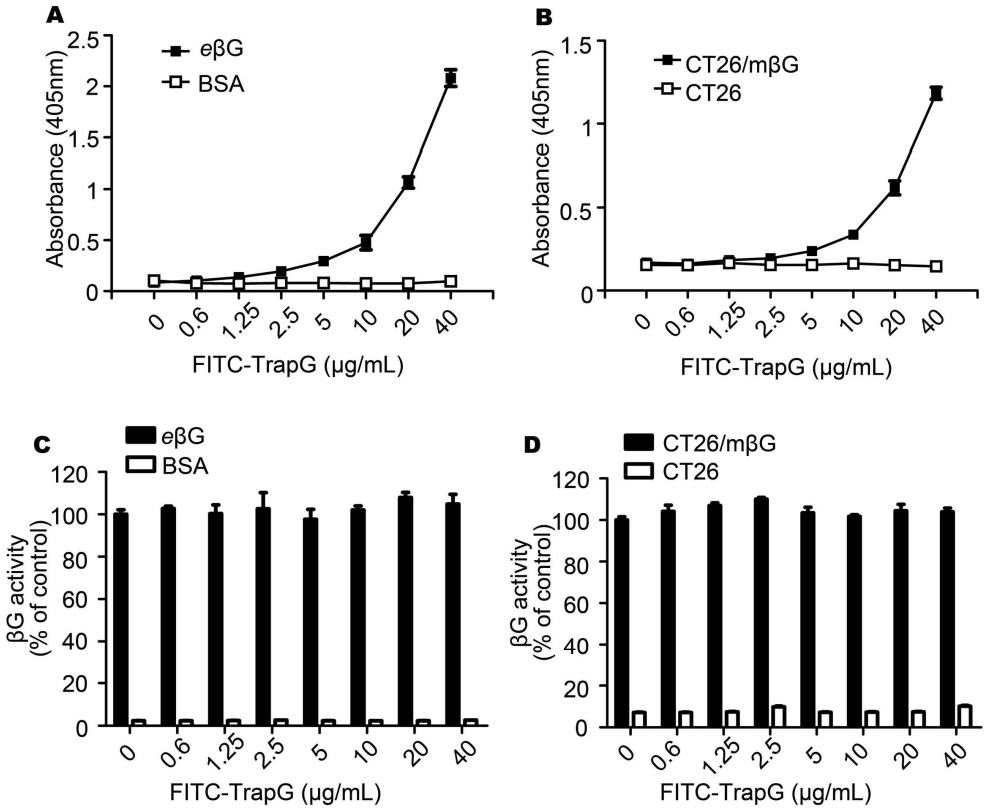

Figure 2. βG-specific activation of FITC-TrapG in vitro. Graded amounts of FITC-TrapG were incubated with (A) βG (filled squares) or BSA (open squares) or (B) CT26/mβG (filled squares) or CT26 (open squares) precoated in the wells of a microtiter plate. Activation and trapping of FITC-TrapG was determined by ELISA using an anti-FITC antibody. After FITC-TrapG treatment, βG activity was determined by hydrolysis of p-NPG substrate in (C) purified proteins (eβG, BSA) or (D) cells (CT26/mβG, CT26).
99x83mm (600 x 600 DPI)

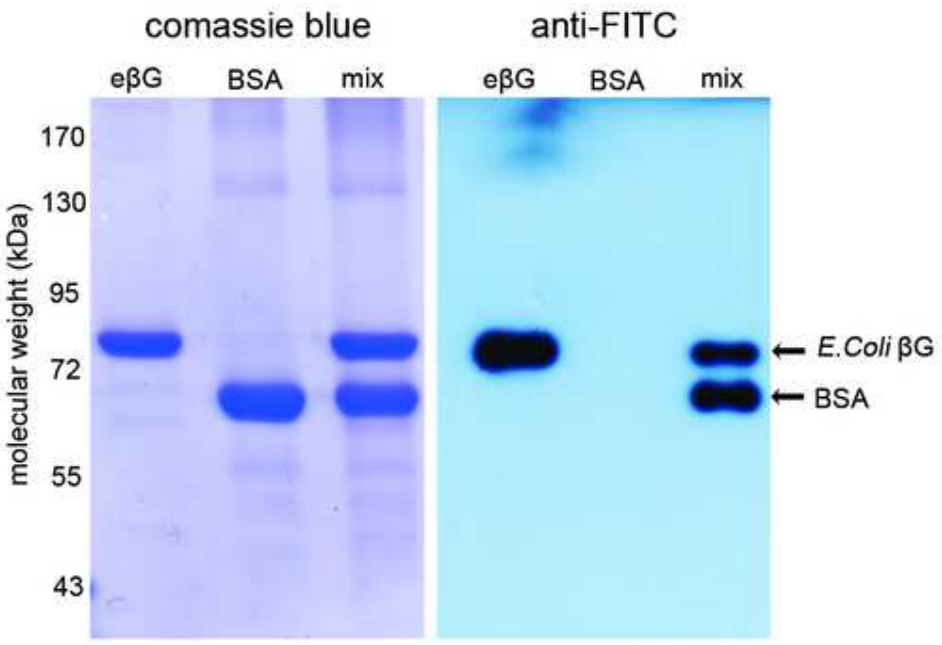

Figure 3. Bystander trapping by FITC-TrapG. FITC-TrapG was incubated with eβG, BSA or a mixture of eβG and BSA. Activation and trapping of FITC-TrapG to proteins was detected by Western blotting using an anti-FITC antibody (right panel). Protein loading was visualized by Coomassie blue staining (left panel).
44x28mm (300 x 300 DPI)

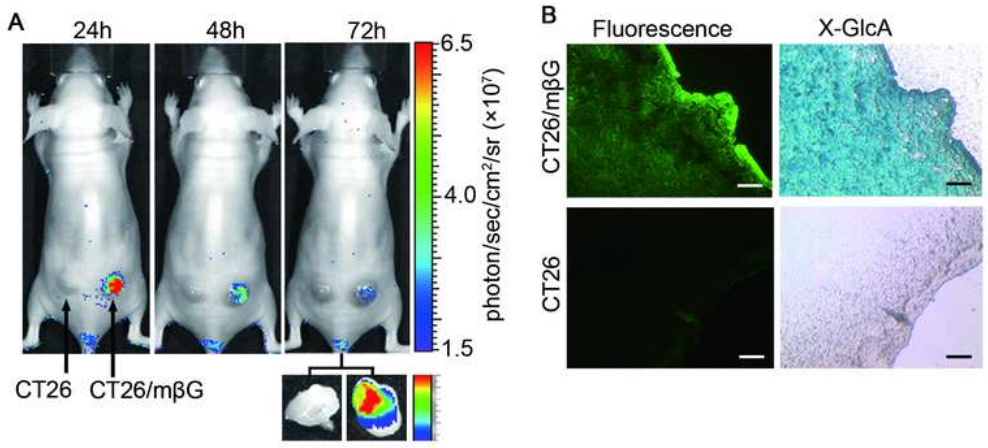

Figure 4. Specific activation of FITC-TrapG in vivo. FITC-TrapG was intravenously injected to BALB/c nude mice bearing CT26/mβG (right flank) and CT26 (left flank) tumors. (A) In vivo optical imaging of FITC-TrapG at 24, 28, 72 hours after probe injection. Tumor tissue was also harvested to confirm specific fluorescent signals. (B) CT26/mβG and CT26 tumors were resected at 24 hours after FITC-TrapG injection, stained with X-GlcA and examined under bright field and fluorescent field illumination. Scale bar: 100 μm.
65x31mm (300 x 300 DPI)

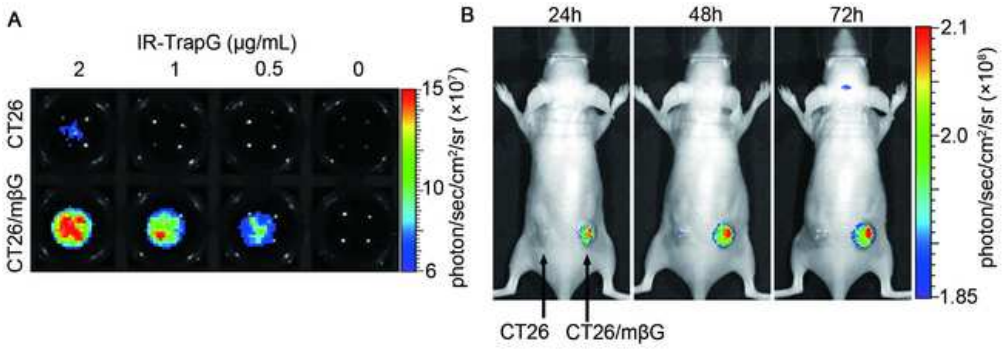

Figure 5. Optical imaging using IR-TrapG. (A) Optical imaging of CT26/mβG or CT26 cells (3×10^6/well) pretreated with 2, 1, 0.5, and 0 μg/ml of IR-TrapG. (B) Optical imaging of subcutaneous CT26/mβG and CT26 tumors in mice at 24, 28, 72 hours after probe injection.
54x20mm (300 x 300 DPI)

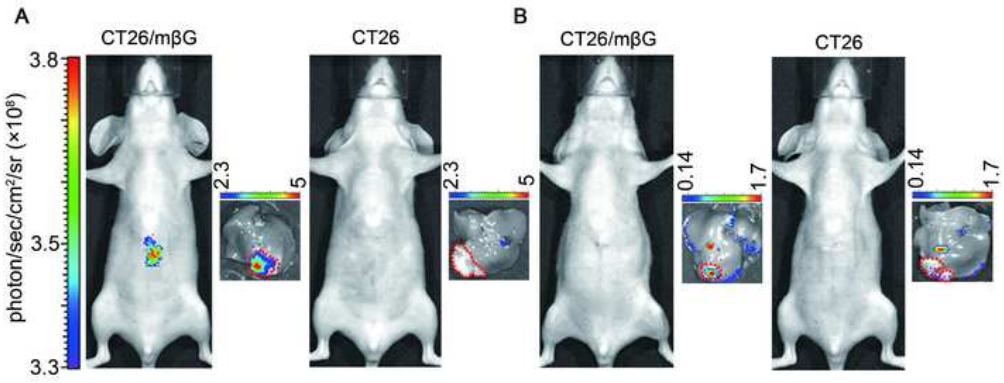

Figure 6. Deep tissue imaging of βG-expressing tumors using IR-TrapG. IR-TrapG or FITC-TrapG was injected into BALB/c mice bearing CT26 or CT26/mβG tumor transplants in livers. Noninvasive optical imaging of (A) IR-TrapG or (B) FITC-TrapG was performed at 24 hours after probe injection. Livers were harvested to confirm location of tumors and specificity of the fluorescent signal. Red dotted lines indicate tumor locations in the liver.
59x24mm (300 x 300 DPI)

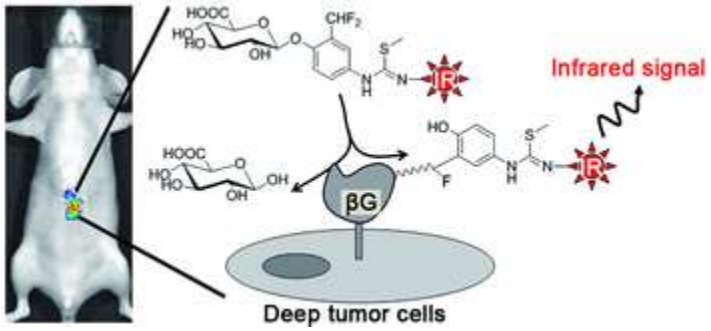

Table Of Contents
29x13mm (300 x 300 DPI)